Radiologic Features of Primary Intracranial Myxomas from the Skull Base: 14 Case Reports and Literature Review

Xinhua Wei[1], *Tianjing Chang*[2], *Huicong Shen*[2]

BACKGROUND: **Primary intracranial myxomas (PIMs) are extremely rare benign tumors that arise from the skull base. The aim of this study was to characterize the radiologic manifestation of PIMs in a series of 14 cases.**

METHODS: **We reviewed the imaging and clinical data of 14 patients with pathologically proven PIMs. Assessed features of lesions include shape, margin, bony destruction, attenuation and/or signal intensity, and pattern of enhancement.**

RESULTS: **Extremely high-density foci indicating calcification or bony debris within the tumors were observed in 5 cases on computed tomography images. On magnetic resonance images, the tumors demonstrated heterogeneous hypointensity on T1-weighted images (T1WI) and hyperintensity on T2-weighted images (T2WI). A honeycomb pattern on enhanced T1WIs was observed in 63.6% (7/11) of the cases.**

CONCLUSIONS: **Radiologic findings of PIMs include calcified foci or bone debris on computed tomography, heterogeneous hypointensity on T1WI and predominantly hyperintensity on T2WI, and honeycomb appearance on enhanced T1WI.**

INTRODUCTION

Myxoma is a benign neoplasm derived from primitive mesenchyme.[1] The first report of a myxoma was published in 1871 by Virchow,[2] who described a mucinous tissue of the umbilical cord. Since then, myxomas are appreciated as rare, locally infiltrative, benign tumors of connective tissue that arise in bone as well as somatic soft tissues, most frequently reported in the atrium of the heart and the mandible.[3-5] Only a few cases of primary intracranial myxomas (PIMs) have been described in the literature.[6-8] Unlike secondary intracranial myxomas, caused by metastatic tumor emboli from the heart, myxomas mainly locate in brain parenchyma.[9] Most PIMs are found at the skull base including the temporal bone,[7,10] posterior fossa,[11] sphenoid sinus, or ethmoid bone.[12,13] Most of the case reports of PIMs have focused on describing the clinical or pathological features in the previous literature.[1,6,7,13,14] However, to our knowledge, the radiologic features of the tumors remains unclear.[11] The aim of the present study was to investigate the computed tomography (CT) and magnetic resonance imaging (MRI) features of PIMs by retrospectively analyzing a series of 14 cases, and the related literatures were reviewed.

MATERIALS AND METHODS

Data Search

We reviewed the clinical and imaging data of 14 patients from Beijing Tiantan hospital with histologically proven PIMs from 2003–2013. None of the patients had a history of heart myxoma. Local human research ethics board approval was obtained to review the clinical and imaging records of patients with PIMs.

Imaging Scanning

CT examination was performed on a 16-row multi-slice spiral CT scanner (Sensation 16; Siemens, Erlangen, Germany) by using a standard CT protocol for the head. All MRI scans were undergone by use of one GE 3.0T MR (Signa HDe, GE Healthcare, Milwaukee, Wisconsin, USA) and another Siemens 3.0T (Siemens Trio,

Key words
- Computed tomography
- Magnetic resonance imaging
- Myxomas
- Skull base

Abbreviations and Acronyms
CSF: Cerebrospinal fluid
CT: Computed tomography
MRI: Magnetic resonance imaging
PIM: Primary intracranial myxoma
T1WI: T1-weighted images
T2WI: T2-weighted images

From the [1]*Department of Radiology, Guangzhou First hospital, Second Affiliated Hospital, South China University of Technology, Guangzhou, Guangdong; and* [2]*Department of Neuroradiology, Tiantan Hospital, Capital Medical University, Beijing, China*

To whom correspondence should be addressed: Huicong Shen, M.D. [E-mail: bjttyyshc@126.com]

Citation: World Neurosurg. (2019) 126:e77-e83.
https://doi.org/10.1016/j.wneu.2019.01.174

*Journal homepage: **www.journals.elsevier.com/world-neurosurgery***

*Available online: **www.sciencedirect.com***

1878-8750/$ - see front matter

Table 1. Summary of Clinical Data and Imaging Findings in 14 Patients with Primary Intracranial Myxomas

						CT Findings			MRI Findings				
Number	Age (Years)/ Sex	Location	Symptoms	Size (cm)	Shape	CT (Density)	Calcification/ Debris	Enhancement	T1WI (Intensity)	T2WI (Intensity)	Enhancement	Central Foci	Capsule Sign
1	32/M	Left parasellar area	Impaired vision, dizziness	4.3 X 3.8	Lobulated	N/A	N/A	N/A	Hypo and high	Hyper	Honeycomb	Thorn-like	Yes
2	25/M	Left parasellar area	Headache, diplopia, abducent paralysis	2.6 X 2.6	Round	N/A	N/A	N/A	Hypo and linear iso	Hyper with dot linear hypo	Honeycomb	Eggshell-like	Yes
3	24/M	Left parasellar area	Facial numbness, ptosis, abducent paralysis	3.2 X 3.1	Round	N/A	N/A	N/A	Hypo and linear iso	Hyper with dot and linear iso	Honeycomb	Spotty and linear	Yes
4	51/M	Left parasellar area	Facial numbness, diplopia	3.2 X 1.9	Lobulated	Low and high	Yes	Mild	N/A	N/A	N/A	N/A	N/A
5	32/M	Right paraseller area	Facial numbness, hearing loss, hoarse voice	7.7 X 5.9	Dumb-bell	N/A	N/A	N/A	Hypo and linear iso	Hyper with linear iso	Patchy and honeycomb	Spotty and linear	Yes
6	25/M	Right parasellar area	Diplopia, abducent paralysis	4.6 X 3.1	Dumb-bell	N/A	N/A	N/A	Hypo, linear iso and dot hyper	Hyper with dot and linear iso	Honeycomb	Thorn-like	Yes
7	34/M	Right parasellar area	Headache, memory disturbances	3.0 X 2.4	Lobulated	Low and high	Yes	Mild	N/A	N/A	N/A	N/A	N/A
8	57/F	Left jugular foramen and petrous	Hoarse voice, ptosis, diplopia, hearing loss	3.0 X 3.6	Lobulated	Low	Yes	N/A	Hypo	Hyper with dot and linear iso	Honeycomb	Eggshell-like	Yes
9	26/M	Sphinoid sinus and sellar	Headache, dizziness, impaired vision	7.0 X 4.4	Lobulated	Low	Yes	N/A	Hypo and linear hyper	Hyper with linear iso	Patchy and cystic	Eggshell-like	Yes
10	43/M	Sphenoid sinus and sellar	Impaired vision	5.3 X 3.3	Lobulated	Low and high	Yes	Mild	Hypo and iso	Hyper with linear iso	heter marked	Thorn-like	Yes
11	27/M	Parasellar area	Impaired vision, headache, dizziness	4.0 X 3.9	Round	N/A	N/A	N/A	Hypo and patchy iso	Hyper with patchy iso	Honeycomb	Thorn-like	Yes
12	41/F	Left parasellar area	Diplopia, facial numbness	3.5 X 3.0	Round	N/A	N/A	N/A	Hypo	Hyper with dot iso	Honeycomb	Spotty and linear	Yes
13	32/M	Left jugular foramen and petrous	Hearing loss, dizziness	2.6 X 1.3	Lobulated	Low	Yes	N/A	N/A	N/A	N/A	N/A	N/A
14	48/F	Right jugular foramen	Hearing loss	2.9 X 1.6	Lobulated	Low and iso	Yes	N/A	Hypo and patchy iso	Hyper with patchy iso	Patchy and honeycomb	Spotty and linear	No

T1WI, T1-weighted imaging; T2WI, T2-weighted imaging; M, male; F, female; N/A, not available.

Erlangen, Germany) imaging scanner. Routine spin-echo T1-weighted images (T1WI) and fast spin-echo T2-weighted images (T2WI) were acquired in the axial and coronal planes. T1WI on axial, sagittal, and coronal view were obtained after gadolinium contrast administration.

Imaging Analysis

Image reading was performed by 2 neuroradiologists (X.H.W. and H.C.S.) in consensus. The following imaging features were analyzed by using CT and MRI: 1) location; 2) size of the tumors; 3) morphology; 4) T1- and T2-signal intensity on MRI; 5) density on CT; 6) pattern of enhancement; 7) density on CT (calcification/debris within the tumors); 8) signal density on MRI; and 9) capsule sign.

Of the 14 patients, 3 were women and 11 were men, and age ranged from 24–57 years (mean age, 35.5 years). Among the 14 patients, 11 were evaluated with preoperative brain MRI, 7 underwent CT, and 4 patients had both CT and MRI (Table 1).

Surgical Approach

The surgical approach for each patient was based on the tumor location, size, pathologic features, and extension of the tumor. Frontotemporal or subtemporal-transtentorial was chosen for the parasellar myxoma. Either a suboccipital-paramedian or a cerebellopontine angle approach was considered for tumors from the jugular foramen. For the tumor coming from the sphenoid sinus, a subfrontal-transbasal and an extended subfrontal approach was selected.

RESULTS

Clinical Symptoms

Patients presented with multiple symptoms. The range of symptom duration was 1 day to 10 years with an average of 27 months. Impaired vision was the most common symptom and was present in 6 (42.8%) patients. A total of 4 of 14 (28.5%) patients presented with facial numbness, 4 (28.5%) with headache, 4 (28.5%) with dizziness, 2 (14.2%) with ptosis, and 1 (0.7%) with memory disturbances. Diplopia was found in 4 (28.5%) patients, and abducent paralysis was noted in 4 (28.5%) patients. Unilateral hearing loss occurred in 2 (14.2%) patients and hoarse voice occurred in 2 (14.2%) patients. The main clinical symptoms are summarized in Table 1.

Imaging Findings

The CT and MRI characteristics of the tumors are summarized in the Table 1. The tumors were located at extra-axial regions of the skull base, such as the parasellar area (n = 11) and jugular foramen (n = 3) (Figure 1). The size of the tumors ranged from 2.6–7.7 cm (mean, 3.9 cm) in the largest diameter, and ranged from 1.3–5.9 cm (mean, 3.1 cm) in the smallest diameter. The tumors demonstrated lobulated (n = 7), dumbbell-like (n = 2), mushroom-like (n = 2), and round (n = 3) in the gross appearance.

Of a total of 7 unenhanced CT scans, all tumors demonstrated well-defined margin, and revealed bone erosion with irregular margin (Figure 2). A total of 6 tumors appeared as heterogeneously hypodensity, which was slightly higher than the density of cerebrospinal fluid (CSF). One tumor was heterogeneous iso- to hyper-density. Extremely high-density foci, appeared as patchy, spotty, and eggshell-like (n = 5) in shape, and represented calcification or bone debris within the tumors (Figure 3A). Enhanced studies were available in 3 cases that revealed mild enhancement on the postcontrast CT scans.

On MRI, all tumors exhibited heterogeneous signal intensity on all MRI sequences. Specifically, on T1WIs, PIMs showed heterogeneous hypointensity but slightly higher than the signal of CSF (Figure 3B). On T2WIs, all the tumors displayed predominantly

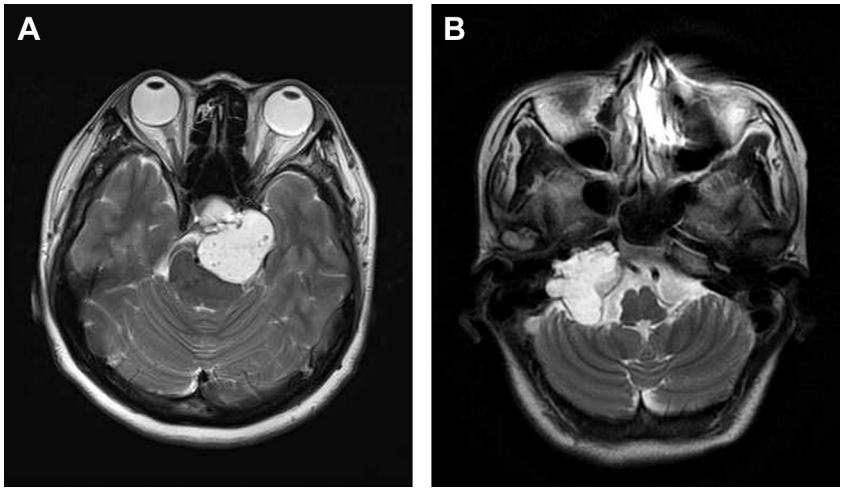

Figure 1. Case 12. Myxoma in a 41-year-old woman. T2-weighted imaging (T2WI) shows a mushroom-like mass locating in the left parasellar area (**A**). Case 14. Myxomas in a 48-year-old woman. A lobulated mass with intense high signal on T2WI located in the right jugular area (**B**).

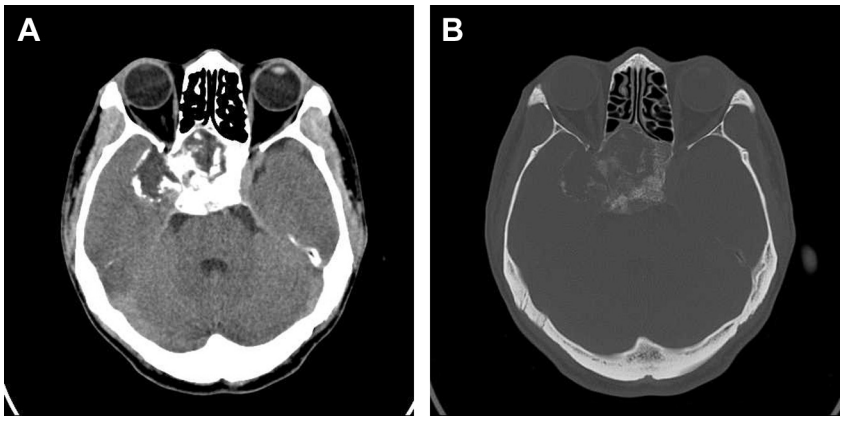

Figure 2. Case 10. Myxoma in a 43-year-old man. Precontrast axial computed tomography scan shows a well-defined mass with heterogeneous attenuation locating in the sphenoid sinus and parasellar region (**A**) and reveals invasive bone destruction in the bone window image (**B**).

hyperintensity, consistent with the signal of CSF in the most part of the tumors (Figure 3C). Additionally, the central part of the tumor had thorn-like (n = 4), spotty (n = 4), and eggshell-like (n = 3) foci with iso or hyperintensity on T1WIs and iso or hypointensity on T2WIs. Discontinuous capsule sign around the tumors displaying linear low signal intensity on T2WIs was observed in 81.8% (9 of 11) cases. On postcontrast images, all the lesions showed heterogeneous enhancement. A honeycomb sign on enhanced T1WIs was observed in 63.6% (7 of 11) tumors that mainly located in parasellar region (Figure 3D). The remaining 4 cases revealed marked heterogeneous enhancement with diffuse linear or spotty low signal. Obvious cystic formation was observed in 1 case.

Postoperative Results

Among the 14 cases, 9 patients received partial tumor resection and 5 tumors were wholly resected. Improvement of clinical symptoms included facial numbness and headache in 5 patients. Unresolved symptoms were reported in 4 cases after surgery. Worsening of preexisting symptoms was found in 1 patient. There were 3 patients who developed new symptoms that included facial paralysis and impaired hearing. Among the 14 cases reviewed, follow-up was unavailable for 9 patients. Four patients had a nearly normal function of cranial nerve after 6 years of follow-up.

Pathology Findings

Histopathology revealed that the lesion consisted of abundant myxoid matrix, among which reticular and collagenous fibers were noted. The cells appeared satellite and spindle with hyperchromatic round or ovoid nuclei, and had a moderate amount of cytoplasm with bands of hyaline tissue (Figure 4A and B). Immunohistochemical staining showed tumor cells reactive for vimentin and negative for S100 protein.

DISCUSSION

PIMs are exceedingly rare benign tumors that originate in mesenchymal tissue, and the etiology of PIMs remains unclear. To the best of our knowledge, no larger case series specifically studied the neuroimaging findings of PIMs. It has been reported that PIMs are most prevalent in patients in the third and fourth decade of life, but can occur at any age.[6] Consistent with previous reports,[9] the mean age of patients in the present study is 35.5 years. The incidence of myxomas is reported nearly equal in men and women.[6] However, this might be attributed to sampling. An obviously male predilection (78.5%, 11/14) was revealed in the present group. In our series, the common locations of the tumors were skull based, such as the parasellar area, jugular foramen, and anterior fossa. Myxomas from the skull base may originate from the primitive mesenchyme in the mastoid, sphenoidal, or ethmoidal cells of embryos and newborns, considering that this particular tissue is responsible for the process of pneumatization.[13,14] It has been reported that myxomas typically manifest with painless, slow growing masses,[1] and when they involve the cranial nerves they can cause symptoms such as impaired vision, facial numbness, and hearing loss. The clinical manifestation of patients with parasellar and clival myxoma commonly present with impaired vision, diplopia, and abducent paralysis. Tumors located at the jugular foramen often cause jugular foramen syndrome, with hoarse voice attributed to this.[14]

Radiologic examination plays a key role in the diagnosis of PIMs. PIMs expand locally, despite their benign character, and they may grow aggressively with bone destruction and remodeling on CT images.[1,15] The tumor appears as well-circumscribed with multilocular compartments. The central area may have a fine, soap-bubble trabeculated surface and less frequently have a honeycomb or tennis-racquet appearance.[5,15,16]

In the present case series, all the cases showed different degrees of bony erosion and revealed irregular margins. In CT scans, the tumors are commonly hypodense. However, tumors arising from the parasellar region commonly display mixed low and extremely high density, which may represent calcification, bone chips, and/or new bone formation.[14] This phenomenon is explained by the makeup of myxoma-undifferentiated mesenchymal cells with the

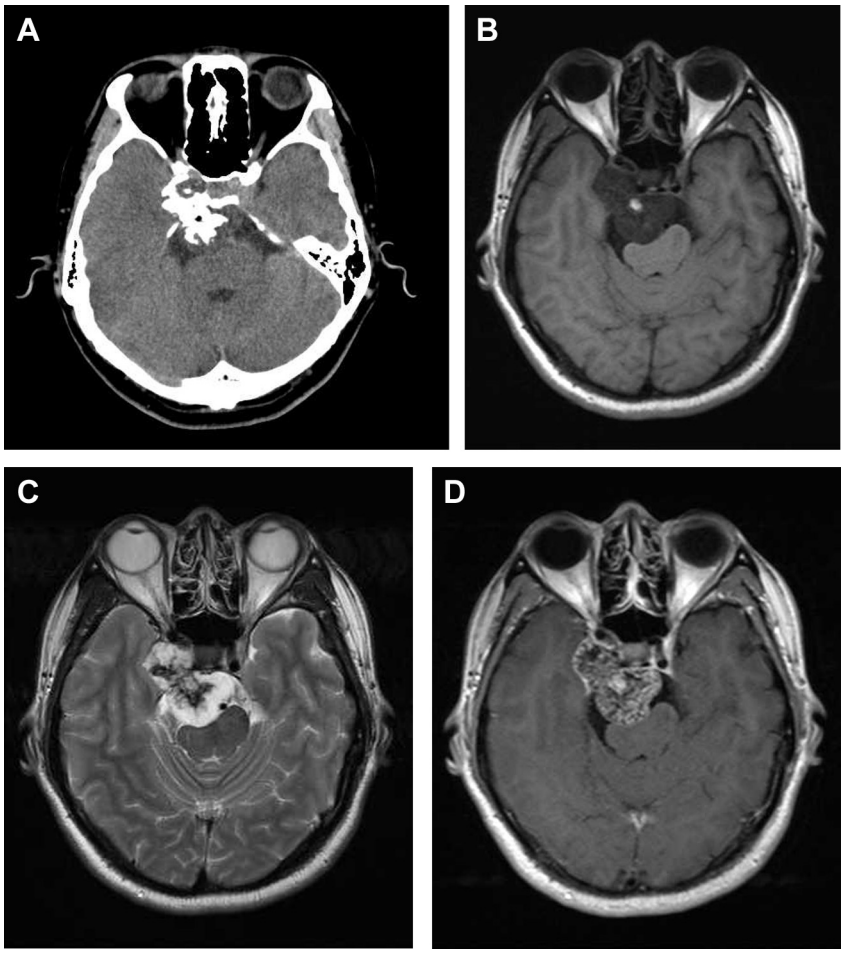

Figure 3. Case 6. Myxoma in a 25-year-old man. Precontrast axial computed tomography scan shows a mass with diffuse calcified foci locating in the right parasellar region (**A**). The mass shows hypointense to the brain gray matter on axial T1-weighted imaging (T1WI) (**B**) and exhibits predominantly marked hyperintense and central mixed-signal foci with thorn-like appearance, as well as linear low signal capsule on T2-weighted imaging (**C**). Postcontrast axial T1WI shows that the mass has characteristic honeycomb enhancement (**D**).

potential to become osteoblasts that form new bone. On MRI, the tumors commonly revealed well-defined masses with variable appearance, such as lobulated, dumbbell-like, mushroom-like, and round in gross shape. Although as a localized tumor, PIMs frequently demonstrated invasive behavior, as evinced by involvement of the sinus and skull base on MRI. These tumors show inhomogenous low signal intensity on T1WIs, and predominantly marked high intensity on T2WIs. However, tumors showed central diffuse spots, linear or coral-like low and/or high signal on both T1WIs and T2WIs. These diffuse foci with inhomogenous signal may represent fibrous, calcification, and irregular osteoid matrix in pathology. The abundant mucoid material in PIMs resulted in the marked high signal intensity on T2WIs. Capsule sign suggesting dura surrounding the tumors exhibiting linier low signal was observed in most of the cases, especially when the tumor was extending into the brain cortex. The tumor was under the dura mater and, therefore, expansion of the tumor resulted in increased tension on the dura mater.[14] Most of the cases in this group displayed incomplete surrounding capsule, which means the tumor is infiltrating into the bone. As the loss of shaping by intact dura mater, the tumor surface became irregular and lobulated.[14] Heterogeneous enhancement from a mild to an intense degree is a frequent finding in PIMs. Specifically, the pattern of honeycomb was characteristic in postcontrast MRI. This phenomenon is explained by the affluent capillary vessels. Despite a poor blood supply, PIMs were found to have affluent capillary vessels in the interstitial tissue, creating nonhomogeneous enhancement on MRI. Honeycomb

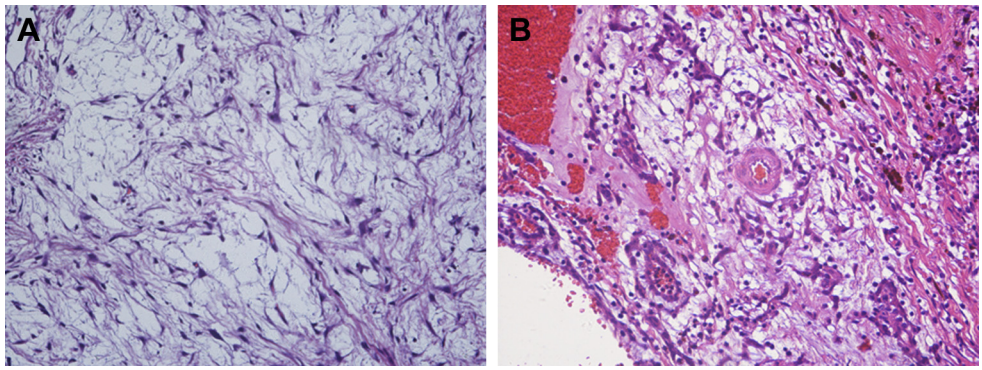

Figure 4. High power (200×) hematoxylin and eosin stain shows myxomatous components composed of scattered stellate or fusiform cells among abundant myxoid matrix (**A**). High power (200×) hematoxylin and eosin stain reveals scattered tumor cells and thin walled vessels within myxoid matrix (**B**).

sign was more commonly seen in the tumors arising in the parasellar regions. However, similar to a study before,[14] the pattern of enhancement was somewhat different when tumors were located in other regions. For instance, in the present series, tumors arising from the jugular foramen displayed inhomogeneous intense enhancement in postcontrast images. One case located in anterior fossa presented obvious large cystic components within the tumor.

The imaging characteristics of PIMs are not pathognomonic, and the imaging appearance of these tumors resembles several other lesions, such as meningioma, schwannoma, chondrosarcoma, chordoma, and chondroblastic tumors, which demonstrate similar expansile lucent lesions. The phenomenon of center calcification, as seen in myxoma, is barely found in a schwannoma.[14] In addition, an invasive margin was commonly seen in myxoma instead of smooth margin in schwannoma in the skull base.[17] An enhancement tumor with dural tail sign is the key point to distinguish meningioma from myxoma. However, it is difficult to differentiate myxomas from chondroblastic tumors or chordomas arising in the cranial base. Chordomas may originate from embryonic notochord residue in the clivus, thereby showing a midline-growing pattern.[7] Bony erosion is common for their aggressive growth. By contrast, myxomas usually arise from bone joints and grow toward the brain stem.[14] Chondrosarcomas are also expansile and lobulated soft tissue masses with bone resorption. Honeycomb enhancement is also similar in appearance to chondroma on MRI,[18] and thus, sometimes it is difficult to distinguish chondroma from myxomas according the imaging findings.

CONCLUSIONS

PIMs is an infiltrative mass predominantly arising from the skull base. These tumors frequently present calcified high density on CT, low signal intensity on T1WI, marked high signal intensity with mixed shapeless foci on T2WI, and capsule sign on T2WI as well as honeycomb sign on enhanced images. Although radiologic are rare and their imaging findings are rather nonspecific, CT and MRI studies are helpful for preoperative diagnosis and surgical planning in patients with PIMs of the skull base.

REFERENCES

1. Windfuhr JP, Schwerdtfeger FP. Myxoma of the lateral skull base: clinical features and management. *Laryngoscope*. 2004;114:249-254.
2. Virchow R. In: *Die Cellularpathologie in ihrer Begründung auf physiologische und pathologische Gewebelehre*. Berlin: Germany Verlag von August Hirschwald; 1871:53.
3. Ataman M, Sarioglu T, Ayas K. Myxoma of the mandible. *Int J Pediatr Otorhinolaryngol*. 1993;27:183-186.
4. Batsakis JG. Myxomas of soft tissues and the facial skeleton. *Ann Otol Rhinol Laryngol*. 1987;96:618-619.
5. Andrews T, Kountakis SE, Maillard AA. Myxomas of the head and neck. *Am J Otolaryngol*. 2000;21:184-189.
6. Menon RK, Goel A, Shah A, Goel N, Rajashekharan P. Primary intracranial myxoma of the parietal region. Illustrated case report. *J Neurooncol*. 2008;88:157-160.
7. Oruckaptan HH, Sarac S, Gedikoglu G. Primary intracranial myxoma of the lateral skull base: a rare entity in clinical practice. *Turk Neurosurg*. 2010;20:86-89.
8. Mueller OM, van de Nes JA, Wieland R, Schoch B, Sure U. Surgical treatment of primary intracranial myxoma in a child following radiotherapy: case report and review of the literature. *Childs Nerv Syst*. 2010;26:829-834.
9. Liu A, Wang CC. Primary myxomas of the skull base. *J Clin Neurosci*. 1996;3:29-33.
10. Osterdock RJ, Greene S, Mascott CR, Amedee R, Crawford BE. Primary myxoma of the temporal bone in a 17-year-old boy: case report. *Neurosurgery*. 2001;48:945-947 [discussion: 947-948].
11. Klein MV, Schwaighofer BW, Sobel DF, Hesselink JR. Primary myxoma of the posterior fossa. *Neuroradiology*. 1990;32:250-251.
12. Moore BA, Wine T, Burkey BB, Amedee RG, Butcher RB 2nd. Sphenoid sinus myxoma: case

report and literature review. *Ochsner J*. 2008;8:166-171.

13. Yin H, Cai BW, An HM, You C. Huge primary myxoma of skull base: a report of an uncommon case. *Acta Neurochir (Wien)*. 2007;149:713-717.

14. Zhang L, Zhang M, Zhang J, et al. Myxoma of the cranial base. *Surg Neurol*. 2007;68(suppl 2):S22-28.

15. DeFatta RJ, Verret DJ, Ducic Y, Carrick K. Giant myxomas of the maxillofacial skeleton and skull base. *Otolaryngol Head Neck Surg*. 2006;134:931-935.

16. Sato H, Gyo K, Tomidokoro Y, Honda N. Myxoma of the sphenoidal sinus. *Otolaryngol Head Neck Surg*. 2004;130:378-380.

17. Hamilton JD, Demonte F, Ginsberg LE. Imaging of carotid canal sympathetic plexus schwannoma. *AJNR Am J Neuroradiol*. 2011;32:1212-1215.

18. Bingaman KD, Alleyne CH Jr, Olson JJ. Intracranial extraskeletal mesenchymal chondrosarcoma: case report. *Neurosurgery*. 2000;46:207-211 [discussion: 211-202].

Conflict of interest statement: The authors declare that the article content was composed in the absence of any commercial or financial relationships that could be construed as a potential conflict of interest.

Received 16 June 2018; accepted 19 January 2019

Citation: World Neurosurg. (2019) 126:e77-e83.
https://doi.org/10.1016/j.wneu.2019.01.174

Journal homepage: ***www.journals.elsevier.com/world-neurosurgery***

Available online: ***www.sciencedirect.com***